ALGORITHM FOR DERIVING SEA SURFACE CURRE NT IN THE SOUTH CHINA SEA

Nurul Hazrina Idris[a] and Mohd Ibrahim Seeni Mohd[b]

[a]Department of Remote Sensing, Faculty of Geoinformation Science and Engineering, Universiti Teknologi Malaysia,81310 Skudai,Johor Darul Takzim,Malaysia- nurulhazrina@fksg.utm.my
[b]Department of Remote Sensing, Faculty of Geoinformation Science and Engineering, Universiti Teknologi Malaysia,81310 Skudai,Johor Darul Takzim,Malaysia- mism@fksg.utm.my

KEY WORDS: Altimetry, Geostrophic current, South China Sea, Tidal current, Wind-driven surface current.

ABSTRACT:

Jason-1 satellite altimetry data are very useful for providing information about the ocean globally in a continuous manner, including the information of sea surface currents. The main objective of the study is to identify the most appropriate algorithm to determine surface current in the South China Sea. The algorithms used to derive sea surface current are geostrophic current algorithms, wind-driven current algorithms and tidal current. The methodology of the study involves the use of sea level height and sea surface wind speed data from Jason-1 satellite altimeter to derive geostrophic current and wind-driven current. Tidal amplitudes from co-tidal chart are used to derive tidal current. The derived surface currents were used to produce combined geostrophic and wind-driven current, combined geostrophic and tidal current and total surface current which is the combination of geostrophic current, wind-driven current and tidal current. Regression analysis with ground truth data were carried out to identify the suitable algorithm of surface current for the South China Sea. The results of analysis indicate that total surface current speed and direction are highly correlated with the ground truth data with correlation of 0.9 and 0.84 respectively. In conclusion, Jason-1 satellite altimetry combined with tidal data to derive the total surface current is appropriate to determine sea surface current circulation pattern in the South China Sea.

1. INTRODUCTION

The South China Sea is a large marginal sea situated at the western side of the tropical Pacific Ocean. It is a semi-closed ocean basin surrounded by South China, Philippines, Borneo Island, Indo-China Peninsula and Peninsular Malaysia. This water body connects with the East China Sea, the Pacific and the Indian Ocean through the Taiwan Straits, the Luzon Straits and the Straits of Malacca, respectively (Chung et al., 2000). The study area of this research is from 2^0 to 15^0 north and from 100^0 to 120^0 east (Figure 1).

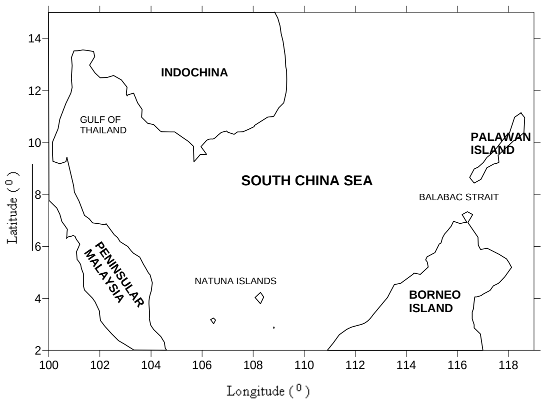

Figure 1. The South China Sea region.

Basically, sea surface current is mainly driven by the density gradient, Coriolis force, wind forcing and tidal forces (Susan et al., 1999). In the South China Sea, geostrophic velocity which is induced by density gradient and Coriolis force is a major component of total surface current velocity. However, the total velocity would be underestimated if only geostrophic velocity is used to represent the total velocity (Chung et al., 2000).

Numerous investigators have studied the surface currents in the South China Sea region. For example, Nurul Hazrina and Mohd Ibrahim Seeni (2007) studied about the sea surface current circulation pattern in the South China Sea derived from satellite altimetry. Peter *et al*. (1999) studied dynamical mechanisms for the South China Sea seasonal circulation and thermohaline variability. Camerlengo and Demmler (1997) simulated the wind-driven circulation off Peninsular Malaysia's east coast. They found that the pile up of water during the northeast (NE) monsoon along Peninsular Malaysia east's coast is greater than during the southwest (SW) monsoon. Moreover, Fang (1997) described the spatial structures of summertime in the southern part of the South China Sea. He found that a large scale wind-driven anticyclonic circulation exists in the upper layer (0~150 m). Fang *et al*.(1997) found that there are four major currents in the upper layer (0~400 m) of the southern part of South China Sea, which are the Nansha Western Coastal Current (NWCC), the Nansha Eastern Coastal Current (NECC), the North Nansha Current (NNC) and the Nansha Counter-wind Current (NCC). They found that the pattern of the currents is different depending on the monsoon period because of the strong influence of the monsoon winds on the Southern South China Sea circulation.

In the work described in this paper, the suitable algorithm to determine surface current in the South China Sea was studied. Geostrophic current (GC) was combined with wind-driven surface current and tidal current to produce combined geostrophic and wind-driven current (G+W), combined geostrophic and tidal current (G+T) as well as total surface current (G+W+T). Analysis was carried out to identify the most suitable algorithm of surface current in the South China Sea. The main data utilized in this study includes the tidal amplitudes from co-tidal chart, the sea level anomaly and the wind speed data from satellite altimetry. Besides, field measurement data obtained from the Japanese Organization Data Center (JODC) was used for analysis purpose. The data are available via the JODC site; http://jdoss1.jodc.go.jp/cgi-bin/1997/ocs. The field measurement data is an average of historical data which was observed from 1953 to 1994 which was measured using the lagrangian buoy.

2. SEA SURFACE CURRENT ALGORITHMS

Algorithms used to estimate the surface currents include the geostrophic current algorithms (Chung *et al*., 2000), the wind-driven current algorithms (Chung *et al*., 2000; Yanagi, 1999) and the tidal current algorithms (Al-Rabeh *et al*., 1990).

2.1 Geostrophic Current Algorithms

Algorithms of geostrophic current are expressed in Equation (1) to Equation (6).

$$u_g = -g / f\,(\delta\zeta / \delta y) \quad (1)$$

$$v_g = g / f\,(\delta\zeta / \delta x) \quad (2)$$

$$\theta_g = tan^{-1}\,(v_g / u_g) \quad (3)$$

$$f = 2\Omega \cos\varphi \quad (4)$$

$$x = R\,(\lambda - \lambda_0) \cos\varphi \quad (5)$$

$$y = R\varphi \quad (6)$$

where u_g and v_g are the geostrophic current in zonal and meridional direction, respectively, θ_g is the geostrophic current direction, g is the gravitational acceleration, f is the Coriolis force, ζ is the sea surface height relative to the geoid, x and y is the local east coordinate and the local north coordinate, respectively, Ω is the Earth rotation rate (7.27 x 10^{-5} s^{-1}), φ is the latitude in radian, λ is the longitude in radian and R is the radius of the Earth (6371 km).

In order to implement the equations, firstly, the Coriolis force, the local east coordinate and the local north coordinates are determined using Equation (4), Equation (5) and Equation (6). Then, derivatives of zonal and meridional direction of sea surface height relative to the geoid are calculated. Then, geostrophic currents in zonal and meridional directions are calculated using Equation (1) and Equation (2). In order to estimate the direction of the geostrophic current, Equation (3) is used.

2.2 Wind-Driven Current Algorithms

Algorithms of wind-driven current are expressed in Equation (7) to Equation (10).

$$u_e = V_0\, exp(az)\, cos(\pi/4 + az) \quad (7)$$

$$v_e = V_0\, exp(az)\, sin(\pi/4 + az) \quad (8)$$

$$V_0 = \tau / (\sqrt{\rho^2 f A_z}) \quad (9)$$

$$a = \sqrt{(f / 2 A_z)} \quad (10)$$

where u_e and v_e are the wind-driven current in zonal and meridional direction, respectively, A_z is the vertical eddy viscosity, f is the Coriolis force, ρ is the water density, τ is the wind stress = $\rho_a C_d W^2$ where ρ_a is the air density, W is the wind speed 10 m above the sea surface and C_d is the drag coefficient (2.6 x 10^{-3}).

In order to implement the equations, firstly, the wind-driven current components in zonal and meridional directions for water level, z = 1 m and z = 15 m are determined. Then, the mean of these two velocities is computed and the vector sums of the components are calculated to obtain the current speeds. This speed is called the wind-driven surface current. In this study, wind-driven current velocities at the water level of 15 m from the sea surface are important because the current movement in this level varies significantly. For example, if wind speed blowing in the water surface is 400 cm s^{-1}, the wind-driven current speed at the water level of 1 m, 15 m and 30 m are 8.5 cm s^{-1}, 2.2 cm s^{-1} and 1.5 cm s^{-1}, respectively. This shows that the difference of wind-driven velocities in 15 m from surface water is 6.3 cm s^{-1} which is significant. However, below the 15 m water level from the sea surface, the current velocity does not change significantly whereby the difference is less than 1 cm s^{-1}.

The equations above indicate that the speed of the wind-driven surface current is proportional to wind stress. According to Ekman spiral theory, the surface water movement is deflected by $\pi/4$ to the wind direction. In the northern hemisphere, the wind-driven surface current is deflected in a clockwise direction. This is because of the force balance between the wind drag and the water drag (Yanagi, 1999). Therefore, in this study, the direction of wind-driven current (θ_e) is estimated by adding 45^0 clockwise to the direction of the surface wind.

2.3 Tidal Current Algorithms

Algorithms of tidal current are expressed in Equation (11) to Equation (13).

$$\delta u_t / \delta t - (\delta / \delta z(A_v\, \delta u / \delta z)) - fv = -g\, \delta\eta / \delta x - (1/\rho(\delta P / \delta x)) \quad (11)$$

$$\delta v_t / \delta t - (\delta / \delta z(A_v\, \delta v / \delta z)) + fu = -g\, \delta\eta / \delta y - (1/\rho(\delta P / \delta y)) \quad (12)$$

$$\theta_t = tan^{-1}\,(v_t / u_t) \quad (13)$$

where u_t and v_t are the zonal and meridional tidal currents, respectively, f is the Coriolis force, g is the gravitational acceleration, η is the tidal amplitudes, A_v is the vertical eddy viscosity, x and y is the local east coordinate and the local north coordinate, respectively, t is the time, P is the atmospheric pressure, ρ is the water density, z is the water level and θ_t is the tidal current direction.

In order to implement the algorithms of tidal current, firstly, tidal current in zonal and meridional direction is determined using Equation (11) and Equation (12). Then, the direction of tidal current is determined using Equation (13).

In this study, the combination of geostrophic and tidal current was derived by combining the u and v values of geostrophic current and tidal current. Besides, the combination of geostrophic and wind-driven current also was derived by combining the u and v values of geostrophic current and wind-driven current. Finally, the total surface current were estimated by combining the u and v values of geostrophic current, wind-driven current and tidal current.

3. RESULTS AND ANALYSIS

Table 1 and Table 2 indicate some of the results of the derived sea surface current speed and direction, respectively. In order to investigate the accuracy of geostrophic current, combined geostrophic current and wind-driven surface current, combined geostrophic current and tidal current as well as total surface current derived from the equations, the correlation coefficient with ground truth values was computed. The total number of samples used were 50 points. Figure 2 illustrates the regression lines of derived surface current speed and direction with ground truth data.

LAT (^{0})	LONG (^{0})	GROUND DATA (cm s^{-1})	DERIVED SURFACE CURRENT SPEEDS (cm s^{-1})			
			GC	G+W	G+T	G+W+T
4	111	15.4	16.6	13.2	11	10.6
6	107	5.1	4.7	7.2	3.4	5.5
7	115	5.1	10.3	9.3	10.3	9.3
8	106	10.3	4.8	7	7	9.8
8	104	5.1	7.8	7.8	7.8	7.8
8	111	15.4	3.1	6.8	3.1	6.8
9	107	5.1	1.4	5.5	6.9	7.8
9	110	15.4	4.3	7.4	4.3	7.4
9	112	5.1	1.3	5.4	1.3	5.4
10	108	10.3	3.8	8.9	5.4	8.3
11	114	5.1	3.5	5.1	3.5	5.1
11	109	5.1	8.5	11.2	4.5	7.6
12	110	15.4	4.3	6	4.3	6
12	112	10.3	7.2	7.1	7.2	7.1
12	112	15.4	14.3	13.4	14.3	13.4

GC = Geostrophic current
G+W = Combined geostrophic and wind-driven current
G+T = Combined geostrophic and tidal current
G+W+T = Total surface current

Table 1: Speed of derived surface current and ground truth data.

LAT (^{0})	LONG (^{0})	GROUND DATA (^{0})	DERIVED SURFACE CURRENT DIRECTIONS (^{0})			
			GC	G+W	G+T	G+W+T
4	111	281	261	260	290	279
6	107	265	254	271	241	257
7	115	242	176	228	176	228
8	106	357	298	304	290	297
8	104	284	332	326	250	273
8	111	332	321	300	321	300
9	107	239	125	212	227	251
9	110	357	341	305	341	305
9	112	160	132	206	132	206
10	108	79	8	54	47	64
11	114	253	236	253	236	253
11	109	58	33	66	29	52
12	110	34	51	40	51	40
12	112	272	296	298	296	298
12	112	120	114	92	114	92

GC = Geostrophic current
G+W = Combined geostrophic and wind-driven current
G+T = Combined geostrophic and tidal current
G+W+T = Total surface current

Table 2: Direction of derived surface current and ground truth data.

It was found that the derived surface currents have good agreement with the ground truth data whereby the correlation coefficient in 95 percent confidence interval is more than 0.5. As far as the derived geostrophic current was concerned, the accuracy of surface current speed was much better than the direction with 0.86 and 0.72, respectively. However, when the geostrophic current was combined with the wind-driven current, the accuracy improved to 0.88 and 0.82 for the speed and direction, respectively. When the geostrophic current was combined with the tidal current, the accuracy of speed and direction are 0.82 and 0.80, respectively. As far as the accuracy of total surface current was concerned, the accuracy of speed and direction was improved considerably to 0.9 and 0.84, respectively.

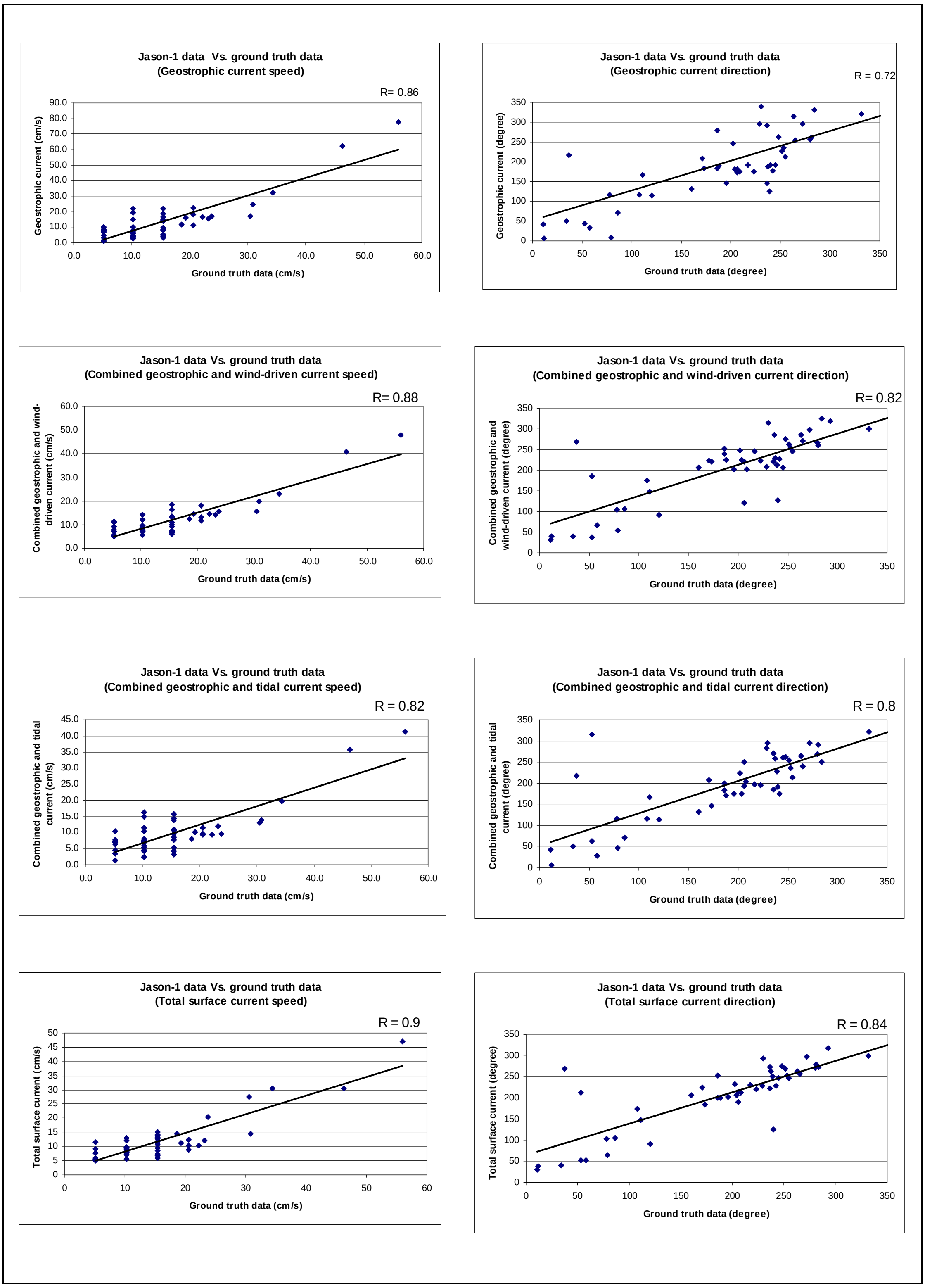

Figure 1: Regression lines between the derived surface current speed and direction with ground truth data.

4. CONCLUSIONS

Total surface current can be estimated using the sea surface height data and wind data derived from satellite altimeter in conjunction with field data. It was found that the derived total surface current is well correlated with the field data whereby the correlation coefficient for the speed and the direction are 0.9 and 0.84, respectively. This leads to the conclusion that the surface current in the South China Sea can be estimated using the combination of geostrophic current, wind-driven current and tidal current.

REFERENCES

Al-Rabeh, A. H., Gunay, N., and Cekirge, H. M., 1990, A hydrodynamic model for wind-driven and tidal circulation in the Arabian Gulf. *Applied Mathematical Modelling*, **14**, pp 410 – 419.

Camerlengo, A., and Demmler, M. I., 1997, Wind-driven circulation of Peninsular Malaysia's eastern continental shelf. *Scientia Marina*, **61**, pp 203–211.

Chung, R. H., Zheng, Q., Soong, Y. S., Nan, J. K., and Jian, H. H., 2000, Seasonal variability of sea surface height in the South China Sea observed with TOPEX/Poseidon altimeter data. *Journal of Geophysical Research*, **105**, pp 13,981-13,990.

Fang, W. D., 1997, Structures of summer circulation in Southern South China Sea. *Nanhai Studia Marina Sinica*, **12**, pp 217-223 (in Chinese with English abstract).

Fang, W. D., Guo, Z. X., and Huang, Y. T., 1997, Observation and study on the circulation in the southern South China Sea. *Chinese Science Bulletin*, **42**, pp 2264-2271 (in Chinese).

Nurul Hazrina Idris and Mohd Ibrahim Seeni Mohd, 2007, Sea surface current circulation pattern in the south china sea derived from satellite altimetry. Proceeding of Asian Conference on Remote Sensing, Kuala Lumpur, Malaysia.

Peter, C. C., Nathan, L. E., and Chenwu Fan, 1999, Dynamical mechanism for the South China Sea seasonal circulation and thermohaline variability. *Journal of Physical Oceanography*, **29**, pp 2971- 2989.

Susan, D., Antczak, T., Leben, R., Born, G., Barth, S., Cheney, R., Foley, D., Goni, G. J., Jacobs, G., and Shay, N. 1999, Altimeter data for operational use in the marine environment. Oceans '99. Mts/IEEE.

Yanagi, T., 1999, Coastal oceanography. Terra Scientific Publishing Company, Tokyo and Kluwer Academic Publisher, Dordrecht, London, Boston.

ACKNOWLEDGEMENTS

The Jason-1 satellite data were processed by SSALTO/DUACS and distributed by Archiving, Validation, and Interpretation of Satellite Data in Oceanography Centre (AVISO), with support from National d'Etudes Spatiales (CNES), France. The field measurement data were provided by the Malaysian Meteorological Services and Japanese Organization Data Centre. We are also grateful to Professor T. Yanagi and Japan Society for Promotion of Science (JSPS) for their contributions.